Commun. Theor. Phys. **75** (2023) 025403 (12pp) https://doi.org/10.1088/1572-9494/acaaf5

Relativistic models of anisotropic superdense star in the regime of Karmarkar's condition

Bikram Keshari Parida[1], Shreya Majumder[2], Shyam Das[3], Koushik Chakraborty[4] and Farook Rahaman[5,*]

[1] Department of Physics, Pondicherry University, Kalapet, Puducherry 605014, India
[2] Department of Physics, North Bengal St. Xavier's College, Jalpaiguri, West Bengal, 735135, India
[3] Department of Physics, Malda College, Malda 732101, West Bengal, India
[4] Department of Physics, Government College of Education, Burdwan, West Bengal, 712103, India
[5] Department of Mathematics, Jadavpur University, Kolkata 700 032, West Bengal, India

E-mail: parida.bikram90.bkp@gmail.com, shreya.mjmdr@gmail.com, shyam_das@associates.iucaa.in, koushik@associates.iucaa.in and rahaman@associates.iucaa.in

Received 31 August 2022, revised 9 December 2022
Accepted for publication 13 December 2022
Published 23 February 2023

Abstract

We obtained a new class of solutions for a relativistic anisotropic compact star by utilizing the Karmarkar embedding condition. To obtain the closed-form solution a suitable form of one of the gravitational potentials has been chosen to determine the other by analyzing the Karmarkar condition. The resulting solutions are found to be well-behaved and regular and could describe a compact stellar object. Considering the current estimated values of the mass and radius of the pulsar $4U1820-30$ as input parameters, all the physically relevant parameters are shown to be well-behaved to a very good degree of accuracy.

Supplementary material for this article is available online

Keywords: anisotropic compact star, embedding class one, Karmarkar's condition

1. Introduction

Scientists have been amazed by the relativistic compact objects over the last few decades. Towards the end of their lifetime, stars having an initial mass larger than Chandrasekhar's limit collapse to form compact objects. When gravity overpowers the pressure due to neutron degeneracy, the situation leads to the formation of neutron stars. On the other hand, in white dwarf stars, the effect of gravity is balanced by the pressure due to electron degeneracy. In the year 1916, for the first time, Schwarzschild [1] obtained the exact solution of static spherically symmetric compact objects in hydro-static equilibrium which has the vacuum exterior gravitational field. After that, many researchers continuously investigated the exact solution of compact stellar objects. The nature of the matter composition and distributions of the star decides its interior geometry and hence the structure as a whole. The interior geometry and nature of the compact stellar configuration can be known by assuming a particular suitable metric potential and solving the Einstein field equations. But finding a suitable metric potential that satisfies all the regularity condition is an extremely difficult job. For the modelling of the realistic compact stellar object, the search for the exact solution of the Einstein field equations has been an intense area of relativistic astrophysics.

Usually, for the study of compact stellar structure in the general relativity context, the isotropic nature of the matter distribution has been considered, i.e. people have considered the perfect fluid which has equal tangential (p_t) and radial (p_r) pressures. But in reality, the anisotropy in the interior of the stellar structure can arise because of many reasons. In a compact object, whenever the pressures in the radial and tangential directions are not the same they produce anisotropy. Since the paper by Bowers and Liang [2], in the context of general relativity, there has been ample research in the study of the role of anisotropy in a relativistic star. The geometry of spacetime inside the star matches the Schwarzschild geometry outside the star. The extremely

* Author to whom all correspondence should be addressed.

dense matter inside the compact star is relativistic. When the density becomes of the order of $10^{15}\mathrm{gm}-\mathrm{cm}^{-3}$, local anisotropy may arise inside the star [3]. Kippenhahn and Weigert [4] indicated that anisotropy can be introduced by the existence of a type 3A superfluid or by the presence of a solid stellar core. Anisotropy can also be possible because of the different kinds of phase transitions (Sokolov [5]) or pion condensation (Sawyer [6]). In the framework of a relativistic anisotropic fluid, Herrera and Santos [7] investigated the influences of slow rotation in stars, and Letelier [8] studied the mixture of two gases, such as ionized hydrogen and electrons. Weber [9] illustrated that strong magnetic fields act as a means for generating anisotropy in pressure inside a compact and spherical object. For a typical polytropic index, Thirukkanesh and Ragel [10] determined exact solutions to Einstein's field equations for a spherically symmetric distribution of anisotropic matter. Researchers [11–13] explored various aspects of polytropic EOS in the studies of a static perfect fluid sphere. Thirukkanesh and Ragel [14] have employed modified Van der Waals EOS to characterise charged fluid spheres having anisotropic pressure. Wormholes [15] and gravastars [16, 17] are also considered anisotropic. Recently, the effect of tidal deformation has also been studied by considering the anisotropic matter distributions [18–20]. Gedela *et al* [21] presented a core-envelope model of an anisotropic star. A three-layered model of a compact star was reported by [22]. Therefore, it is important to study the nature of the space-time of anisotropic fluid spheres under the general theory of relativity.

The necessary and sufficient condition to embed a 4-dimensional spherically symmetric space in a 5-dimensional space was proposed by Karamakar [23]. This condition can be expressed as a simple equation of the components of the Riemannian curvature tensor. Many researchers used this condition for general relativistic studies of compact stars [22, 24–28]. Some researchers [24, 25, 27, 29–32] modelled anisotropic stars using Karmakar's condition. Using this nice condition, the charged anisotropic star was modelled by [33–35]. Deb *et al* [36] proposed a new model of a compact star under $f(T)$ gravity in which they utilized this condition to find out one of the metric potentials. Recently, Pant *et al* [26, 37] used the technique of gravitational decoupling in their model for the charged compact star. They have considered an embedding class I type spacetime. Inspired by some earlier research investigations, in this present paper, we explore static anisotropic fluid solutions of Einstein Field equations in the framework of Karmarkar's condition that could describe observationally compatible compact stellar objects. In particular, we explore the well-known pulsar $4U1820-30$. To construct the model, we have assumed a specific type of metric potential g_{rr}. This particular form of the metric potential was obtained by Das *et al* [38] in developing a compact stellar model under a specific anisotropic profile. Then using the famous Karmakar's embedding class—I condition and the form of metric g_{rr}, we calculated the expression for g_{tt}. All the physical parameters are well-behaved and regular inside the anisotropic star which implies a realistic description of astrophysical compact objects.

In the present paper, we use that metric to develop models of the dense compact star under the well-known Karmakar condition. More specifically, we are interested in whether this particular geometry can generate the static stellar model of compact objects and it is found that under the Karmakar condition, it is possible to obtain the stellar model. Another interesting point of this model is that under certain conditions between model parameters (α, β, R), the assumed metric potential reduces to the well-known Tolman metric. The assumed metric potential which reduces to the Tolman solution with suitable fixation of model parameters represents a compact stellar structure.

This paper is organised as follows. We discuss the Einstein field equations with pressure anisotropy for the compact object in section 2. In section 3, we derive the form of the g_{rr} with the help of the Karmarkar condition. In section 4, we present the new solution. Requirements for a physical solution are described in section 5. The interior solution is matched with the exterior Schwarzschild line element in section 6. Physical analysis of our solution and its compatibility with the observed pulsar are presented in sections 7 and 8. In section 10, the stability of the new model of the compact star is analysed. We conclude with a discussion of the results in section 11.

2. Einstein's equation

Assuming spherical symmetry for the relativistic superdense star, we consider the metric of the following form to describe the geometry inside it with coordinates (t, r, θ. ϕ).

$$\mathrm{d}s^2 = -\mathrm{e}^{\nu(r)}\mathrm{d}t^2 + \mathrm{e}^{\lambda(r)}\mathrm{d}r^2 + r^2(\mathrm{d}\theta^2 + \sin\theta^2\mathrm{d}\phi^2). \quad (1)$$

Here the gravitational potentials, $\nu(r)$ and $\lambda(r)$, are independent of the time coordinate.

We assume that the star is made up of anisotropic matter. The energy-momentum tensor consistent with the matter distribution inside the star is as follows:

$$T_{ij} = (\rho + p)u_i u_j + p_t g_{ij} + (p_r - p_t)\xi_i\xi_j. \quad (2)$$

Here ρ represents the energy density. p_r and p_t are the radial and tangential fluid pressures respectively. u_i represents the 4-velocity of the fluid and ξ^i is a unit space-like 4-vector along the radial direction such that the following conditions are satisfied $u^i u_i = -1$, $\xi^i\xi_j = -1$ and $u^i\xi_j = 0$.

The Einstein field equations corresponding to spacetime metric (13) with $G = c = 1$ written as

$$8\pi\rho = \frac{1}{r^2}(1 - \mathrm{e}^{-\lambda}) + \frac{\lambda'}{r}\mathrm{e}^{-\lambda}, \quad (3)$$

$$8\pi p_r = -\frac{1}{r^2}(1 - \mathrm{e}^{-\lambda}) + \frac{\nu'}{r}\mathrm{e}^{-\lambda}, \quad (4)$$

$$8\pi p_t = \frac{\mathrm{e}^{-\lambda}}{4}\left(2\nu'' + \nu'^2 - \nu'\lambda' + \frac{2\nu'}{r} - \frac{2\lambda}{r}\right), \quad (5)$$

where a prime (') denotes differentiation with respect to r. The anisotropic pressure which is the difference of pressures along transverse and radial directions is given by (using 4 and 5)

$$\Delta(r) = 8\pi(p_t - p_r) = \mathrm{e}^{-\lambda}\left(\frac{\nu''}{2} + \frac{\nu'^2}{4} - \frac{\nu'}{2r} - \frac{\nu'\lambda'}{4} - \frac{\lambda'}{2r} + \frac{\mathrm{e}^{\lambda}-1}{r^2}\right) + \frac{1}{r^2}. \quad (6)$$

The mass contained within radius r of the spherically symmetric distribution of matter is

$$m(r) = \frac{1}{2}\int_0^r \tilde{r}^2\rho \mathrm{d}\tilde{r}. \quad (7)$$

3. Karmarkar condition

In general, a 4-dimensional space can be embedded in a 10-dimensional flat space. Eisenhart showed that a 4-dimensional spherically symmetric space is immersible in a 6-dimensional flat space. Therefore, it is embedded in class II space. Karmakar put forward a condition that is necessary and sufficient to embed a 4-dimensional spherically symmetric space in a 5-dimensional space, thereby making it of class I. In terms of the components of the Riemann curvature tensor, the condition can be expressed as follows:

$$R_{1414}R_{2323} = R_{1212}R_{3434} + R_{1224}R_{1334}, \quad (8)$$

Now, the components of the Riemann curvature tensor for the line element (13) are:

$$\begin{aligned} R_{1414} &= -\mathrm{e}^{\nu}\left(\frac{\nu''}{2} + \frac{\nu'^2}{4} - \frac{\lambda'\nu'}{4}\right),\\ R_{2323} &= -\mathrm{e}^{\lambda}r^2\sin^2\theta(\mathrm{e}^{\lambda}-1),\\ R_{1212} &= \frac{r\lambda'}{2},\\ R_{2424} &= \frac{1}{2}\nu' r\mathrm{e}^{\nu-\lambda},\\ R_{3434} &= R_{2424}\sin^2\theta,\\ R_{1224} &= 0,\\ R_{1334} &= R_{1224}\sin^2\theta = 0. \end{aligned} \quad (9)$$

When all the values of equation (9) are substituted in equation (8), the Karmakar condition reduces to the following form:

$$\frac{2\nu''}{\nu'} + \nu' = \frac{\lambda'\mathrm{e}^{\lambda}}{\mathrm{e}^{\lambda}-1}. \quad (10)$$

It has been pointed out that the above equation (10) is the necessary and sufficient condition for the embedding of class-I when expressed in terms of the curvature components. It is interesting to note that the solution obtained by Pandey and Sharma [39] is not class-I type even though it satisfies the Karmarkar condition.

Integrating equation (10), we get a more simple form of the condition.

$$\mathrm{e}^{\lambda} = 1 + F\nu'^2\mathrm{e}^{\nu}, \quad (11)$$

where F is an arbitrary constant. The Karmarkar condition furnishes a relation between the two metric potentials.

The generating function $\lambda(r)$ thus provides us with a solution to the system as shown in the following section.

4. Generating a new solution

Das *et al* [38] have developed a new class of compact stellar models by choosing a particular metric potential g_{rr} and anisotropy thereby generating the g_{tt} metric solution. Our aim is to develop a realistic model of the compact star. To achieve this end, we assume the metric potential g_{tt} of the form

$$\mathrm{e}^{\nu(r)} = \left(\frac{\alpha}{R^2 - r^2} + \beta\right)^2. \quad (12)$$

The assumed metric potential is finite, continuous, and well-defined inside the star. Now it may be noted that under certain assumptions this metric potential reduces to the well-known Tolman metric [40]. The assumed metric potential can be written as

$$\mathrm{e}^{\nu(r)} = \left[\frac{\alpha}{R^2}\left(1 - \frac{r^2}{R^2}\right)^{-1} + \beta\right]^2. \quad (13)$$

Now if we assume $\frac{r}{R} \ll 1$, the above expression can be written as

$$\mathrm{e}^{\nu(r)} = \left[\frac{\alpha}{R^2}\left(1 + \frac{r^2}{R^2} + \frac{r^4}{R^4} + ...\right) + \beta\right]^2. \quad (14)$$

Expanding and keeping the higher-order terms of $\frac{r}{R}$ up to the order of 4 we have

$$\mathrm{e}^{\nu(r)} = \left(\frac{\alpha^2}{R^4} + \frac{2\alpha\beta}{R^2} + \beta^2\right) + r^2\left(\frac{2\alpha^2}{R^6} + \frac{2\alpha\beta}{R^4}\right) + \frac{\alpha^2}{R^4}\frac{r^4}{R^4}. \quad (15)$$

Now if we set

$$\frac{\alpha^2}{R^4} + \frac{2\alpha\beta}{R^2} + \beta^2 = 1,$$

we have the relation

$$R^2 = \frac{\alpha}{1-\beta}. \quad (16)$$

Now using (16) the expression for $\mathrm{e}^{\nu(r)}$ (equation (15)) turns out as

$$\mathrm{e}^{\nu(r)} = \left[1 + \frac{r^2}{\alpha}(1-\beta)^2\right]^2. \quad (17)$$

Since R is large as compared to r from equation (16) we have

$$\frac{\alpha}{1-\beta} \gg 1, \quad (18)$$

i.e.,

$$\frac{1-\beta}{\alpha} \ll 1. \quad (19)$$

Basically, relations (18) and (19) are the same. In those inequalities, R is the curvature parameter describing the

geometry of the configuration having a dimension of length. The numerical value of R is in general much larger than the radii of pulsars which is evident from the value obtained from matching conditions [38]. Hence, the square of it i.e., R^2 is considered much larger than 1 in equation (18) and equation (19). So, equation (17) can be expanded as

$$e^{\nu(r)} = \left[1 + \frac{2r^2}{\alpha}(1-\beta)^2 + \frac{r^4}{\alpha^2}(1-\beta)^4 + ...\right]. \quad (20)$$

$$p_r = \frac{4\alpha(4\alpha^2 F - 4\alpha\beta F(r^2-R^2) + (r^2-R^2)^3)}{(16\alpha^2 F r^2 + (r^2-R^2)^4)(\beta(r^2-R^2)-\alpha)}, \quad (24)$$

$$p_t = \frac{4\alpha(r^2-R^2)^3}{(16\alpha^2 F r^2 + (r^2-R^2)^4)^2(\beta(r^2-R^2)-\alpha)} \times[(r^2+R^2)(-4\alpha^2 F - (r^2-R^2)^3) + 4\alpha\beta F(r^2-R^2)(3r^2+R^2)], \quad (25)$$

$$\Delta = -\frac{1}{(r^8 - 4r^6R^2 + 6r^4R^4 + R^8 - 4r^2(R^6 - 4F\alpha^2))^2(-\alpha + (r^2-R^2)\beta)} \times[8r^2\alpha(r^6 - 3r^4R^2 + 3r^2R^4 - R^6 + 4F\alpha^2) \times (r^6 - 3r^4R^2 - R^6 + 8F\alpha^2 + 8FR^2\alpha\beta + r^2(3R^4 - 8F\alpha\beta))], \quad (26)$$

Neglecting higher order terms, we have finally

$$e^{\nu(r)} = [1 + Ar^2 + Br^4], \quad (21)$$

where $A = \frac{2}{\alpha}(1-\beta)^2$ and $B = \frac{(1-\beta)^4}{\alpha^2}$.

Here, A and B are constant parameters having dimensions L^{-2} and L^{-4} respectively. Equation (21) is the renowned Tolman metric that is widely used in the modeling of compact stars. The assumed metric potential, e^{ν} reduces to a well-known Tolman metric under certain conditions. In the expression of e^{ν} in equation (15) we can see that if we set

$$\frac{\alpha^2}{R^4} + \frac{2\alpha\beta}{R^2} + \beta^2 = 1$$

which is actually

$$R^2 = \frac{\alpha}{1-\beta}.$$

In equation (16), the metric takes a particular form. This particular relationship between the model parameters α, β, and R of equation (16) in this fashion helps one to reduce the assumed metric equation (13) to the Tolman metric. To have a Tolman-like metric one can restrict model parameters to obey equation (16). With the help of Karmarkar's condition (11) for generating embedded class I solution, we get the following solution for the metric potential, $\lambda(r)$:

$$e^{\lambda(r)} = 1 + \frac{16F\alpha^2 r^2}{(R^2 - r^2)^4}. \quad (22)$$

From equations (3), (4), (5), (6) and (7) we get the following physical quantities

$$\rho = \frac{16\alpha^2 F(16\alpha^2 F r^2 - (r^2-R^2)^3(5r^2+3R^2))}{(16\alpha^2 F r^2 + (r^2-R^2)^4)^2}, \quad (23)$$

$$m(r) = \frac{8\alpha^2 F r^3}{16\alpha^2 F r^2 + r^8 - 4r^6R^2 + 6r^4R^4 - 4r^2R^6 + R^8}. \quad (27)$$

5. Necessary physical conditions for the solution

A feasible stellar solution of the Einstein field equations should obey the conditions listed as follows:

(i) The gravitational potentials and the matter variables should be well-defined at the center and singularity free throughout the star.

(ii) Inside the star, the energy density ρ should be positive and its gradient should be negative, i.e., $\rho \geqslant 0$ and $\frac{d\rho}{dr} \leqslant 0$.

(iii) Inside the star, the radial pressure p_r and the tangential pressure p_t must be positive and their gradients should be negative, i.e., $p_r \geqslant 0$, $p_t \geqslant 0$, $\frac{dp_r}{dr} < 0$, $\frac{dp_t}{dr} < 0$.

(iv) The radian pressure must be zero at the boundary of the star, i.e., at $r = b$. However, the tangential pressure p_t may not vanish at $r = b$. The anisotropy must be zero at the center i.e., $\Delta(r=0) = 0$.

(v) Inside the anisotropic star, the Null Energy Condition and Strong Energy Condition of general relativity must be satisfied. This implies the following conditions: $\rho + p_r \geqslant 0$; $\rho + p_t \geqslant 0$; $\rho + p_r + 2p_t \geqslant 0$.

(vi) Inside the anisotropic star, the speed of sound must be subluminal, i.e., $0 \leqslant \frac{dp_r}{d\rho} \leqslant 1, 0 \leqslant \frac{dp_t}{d\rho} \leqslant 1$. Here we have assumed the speed of light, $c = 1$.

(vii) The metric potentials of the space-time inside the star should smoothly match the external space-time, i.e., the Schwarzschild space-time metric at $r = b$ where b defines the radius of the star.

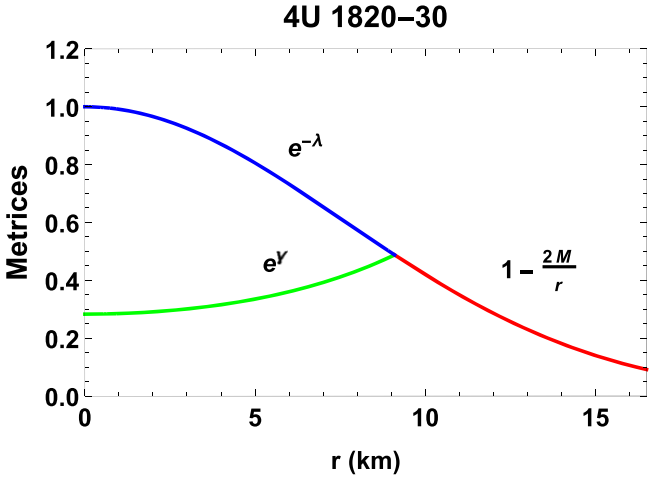

Figure 1. Matching of the metric $e^{\nu(r)}$ and $e^{\lambda(r)}$ with the Schwarzschild exterior metric at the boundary.

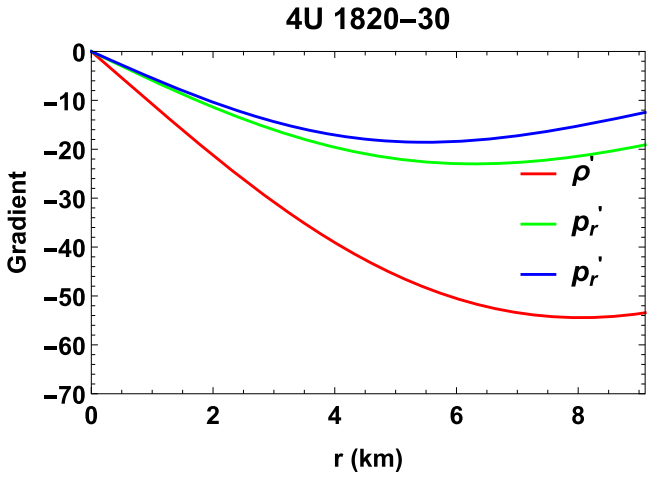

Figure 2. Density and pressure gradients within the star.

6. Matching with exterior space-time

We have considered a static spherically symmetric compact star. Hence the nature of the exterior spacetime may be described by the Schwarzschild line element

$$ds^2 = -\left(1 - \frac{2M}{r}\right)dt^2 + \left(1 - \frac{2M}{r}\right)^{-1}dr^2 + r^2(d\theta^2 + \sin^2\theta d\phi^2). \tag{28}$$

On matching the interior and the exterior spacetime metric at the boundary of the star $r = b$, we get,

$$\left(\frac{\alpha}{R^2 - b^2} + \beta\right)^2 = \left(1 - \frac{2M}{b}\right), \tag{29}$$

$$\left(1 + \frac{16F\alpha^2 b^2}{(R^2 - b^2)^4}\right) = \left(1 - \frac{2M}{b}\right)^{-1}, \tag{30}$$

at boundary, pressure should be zero, $p_r(r = b) = 0$,

$$\frac{4\alpha(4\alpha^2 F - 4\alpha\beta F(b^2 - R^2) + (b^2 - R^2)^3)}{(16\alpha^2 F b^2 + (b^2 - R^2)^4)(\beta(b^2 - R^2) - \alpha)} = 0. \tag{31}$$

Using these boundary conditions, one can calculate the unknown constants in terms of mass and radius of the star as

$$\alpha = \frac{M(b^2 - R^2)^2}{2\sqrt{b^5(b - 2M)}}, \tag{32}$$

$$\beta = \frac{2b^3 - 3b^2 M - MR^2}{2\sqrt{b^5(b - 2M)}}, \tag{33}$$

$$F = \frac{b^3}{2M}. \tag{34}$$

7. Physical analysis

1. From equations (12) and (22), we note that at $r = 0$, $e^{\nu(0)} = \left(\frac{\alpha}{R^2} + \beta\right)^2 = \text{constant}$, $e^{\lambda(0)} = 1$. Thus, the gravitational potentials are finite at the center of the star. We further note that, $(e^{\nu(r)})'_{r=0} = (e^{\lambda(r)})'_{r=0} = 0$. Therefore, the metric potentials are well-behaved everywhere inside the star. Physical features of the metric potentials are shown graphically in figure 1.

2. The expressions for the central density and central pressures are as follows:

$$\rho(0) = \frac{48\alpha^2 F}{R^8},$$
$$p_r(0) = \frac{4\alpha(R^6 - 4\alpha^2 F - 4\alpha\beta F R^2)}{R^8(\alpha + \beta R^2)},$$
$$p_t(0) = \frac{4\alpha(R^6 - 4\alpha^2 F - 4\alpha\beta F R^2)}{R^8(\alpha + \beta R^2)}.$$

Since $\rho(0) > 0$ we have $F > 0$. Moreover, $p_r(0) = p_t(0) > 0$ gives restriction on the model parameters

$$\alpha + \beta R^2 < \frac{R^6}{4\alpha F}.$$

3. The gradient of energy density, radial pressure and tangential pressure are respectively obtained as

$$\frac{d\rho}{dr} = \frac{128\alpha^2 Fr}{(16\alpha^2 Fr^2 + (r^2 - R^2)^4)^3} \times [-64\alpha^4 F^2 r^2 - 4\alpha^2 F(17r^4 + 2r^2 R^2 + 5R^4) + 5(r^2 - R^2)^6(r^2 + R^2)], \tag{35}$$

$$\frac{dp_r}{dr} = \frac{8\alpha r}{(16\alpha^2 Fr^2 + (r^2 - R^2)^4)^2(\alpha + \beta(R^2 - r^2))^2} \times[((r^2 - R^2)^4 + 16Fr^2\alpha^2)(-\alpha + (r^2 - R^2)\beta) \times(3(r^2 - R^2)^2 - 4F\alpha\beta) - ((r^2 - R^2)^4 +16Fr^2\alpha^2)\beta((r^2 - R^2)^3 + 4F\alpha^2 -4F(r^2 - R^2)\alpha\beta) - 4((r^2 - R^2)^3 + 4F\alpha^2)(-\alpha +(r^2 - R^2)\beta)((r^2 - R^2)^3 + 4F\alpha^2 -4F(r^2 - R^2)\alpha\beta)], \tag{36}$$

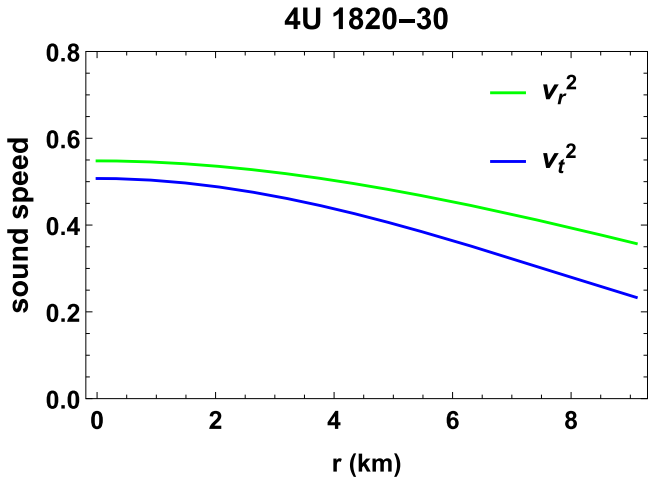

Figure 3. Variation of radial and transverse sound speeds against r.

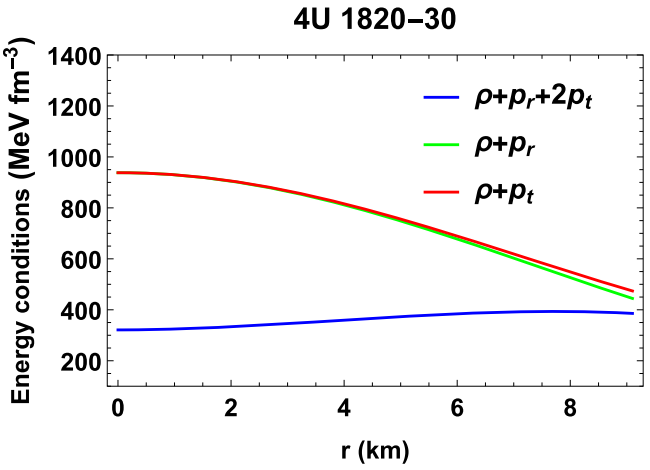

Figure 4. Fulfilment of energy conditions within the stellar interior.

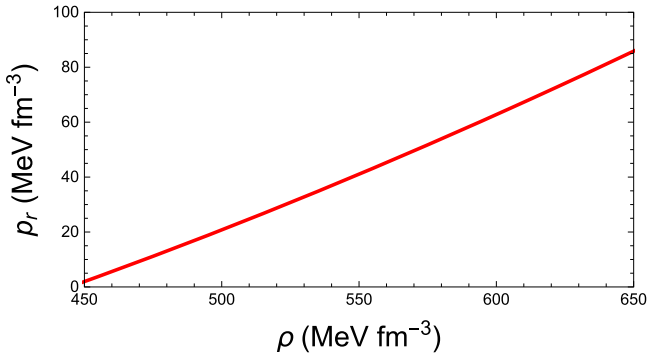

Figure 5. Variation of pressure with density.

$$\frac{\mathrm{d}p_t}{\mathrm{d}r} = \frac{8r(r^2-R^2)^2\alpha}{(16\alpha^2Fr^2+(r^2-R^2)^4)^2(\alpha+\beta(R^2-r^2))^2}$$
$$\times[-(r^2-R^2)^7(r^2+3R^2)\alpha+8F(r^2-R^2)^3$$
$$\times(8r^4+9r^2R^2+7R^4)\alpha^3+128F^2(r^4+r^2R^2+R^4)\alpha^5$$
$$+2(r^2-R^2)((r^2-R^2)^7(r^2+2R^2)-4F(r^2-R^2)^3$$
$$\times(r^4+8r^2R^2+11R^4)\alpha^2-64F^2(5r^4+3r^2R^2$$
$$+2R^4)\alpha^4)\beta+16F(r^2-R^2)^2\alpha$$
$$(-(r^2-R^2)^4(3r^2+2R^2)$$
$$+8F(3r^4+2r^2R^2+R^4)\alpha^2)\beta^2)], \tag{37}$$

As can be noted in figure 2, the above-mentioned physical quantities are all negative inside the star. The nature of the graphs proves that the density, as well as, the radial and tangential pressures are decreasing within the star.

4. The speeds of sound in radial and tangential directions are as follows:

As can be noted from figure 3, sound speeds in both directions lie in the interval [0, 1], where we assume the speed of light, $c=1$. Therefore, the sound speeds are subluminal inside the star.

5. The Null Energy Condition and Strong Energy Condition for the anisotropic star implies the conditions, $\rho+p_r\geqslant 0$,

$$v_r^2 = \frac{1}{16F\alpha(5(r^2-R^2)^6(r^2+R^2)-4F(r^2-R^2)^2(17r^4+2r^2R^2+5R^4)\alpha^2-64F^2r^2\alpha^4)(\alpha+(R^2-r^2)\beta)^2}$$
$$\times[((r^2-R^2)^4+16Fr^2\alpha^2)(((r^2-R^2)^4+16Fr^2\alpha^2)(-\alpha+(r^2-R^2)\beta)(3(r^2-R^2)^2-4F\alpha\beta)$$
$$-((r^2-R^2)^4+16Fr^2\alpha^2)\beta((r^2-R^2)^3+4F\alpha^2-4F(r^2-R^2)\alpha\beta)-4((r^2-R^2)^3+4F\alpha^2)(-\alpha+$$
$$(r^2-R^2)\beta)((r^2-R^2)^3+4F\alpha^2-4F(r^2-R^2)\alpha\beta))], \tag{38}$$

$$v_t^2 = \frac{1}{16F\alpha(5(r^2-R^2)^6(r^2+R^2)-4F(r^2-R^2)^2(17r^4+2r^2R^2+5R^4)\alpha^2-64F^2r^2\alpha^4)(\alpha+(R^2-r^2)\beta)^2}$$
$$\times[(r^2-R^2)^2(-(r^2-R^2)^7(r^2+3R^2)\alpha+8F(r^2-R^2)^3(8r^4+9r^2R^2+7R^4)\alpha^3+128F^2(r^4+r^2R^2$$
$$+R^4)\alpha^5+2(r^2-R^2)((r^2-R^2)^7(r^2+2R^2)-4F(r^2-R^2)^3(r^4+8r^2R^2+11R^4)\alpha^2-64F^2(5r^4$$
$$+3r^2R^2+2R^4)\alpha^4)\beta+16F(r^2-R^2)^2\alpha(-(r^2-R^2)^4(3r^2+2R^2)+8F(3r^4+2r^2R^2+R^4)\alpha^2)\beta^2)]. \tag{39}$$

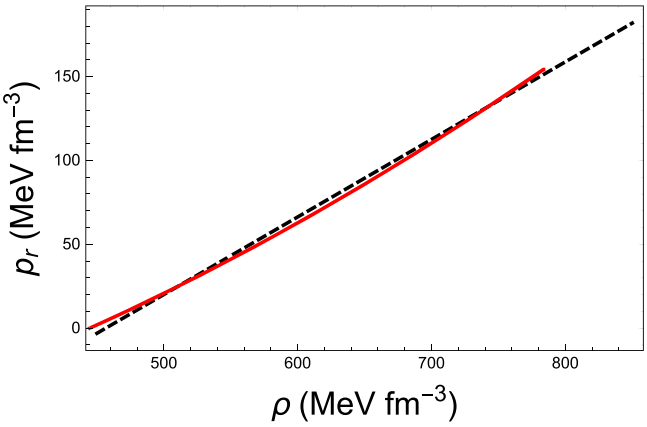

Figure 6. Variation of pressure with density.

$\rho + p_t \geqslant 0$ and $\rho + p_r + 2p_t \geqslant 0$, are satisfied everywhere inside the compact star. Figure 4 shows that the aforementioned energy conditions hold true throughout the star.

6. Figure 1 shows that the metric potentials inside the star nicely match the exterior Schwarzschild metric functions at the boundary.

7. Equation of state of the constituent matter of the star, if assumed to be a perfect fluid, best described as $P = P(\rho)$. In the present study, we have determined the geometry of the compact object. From the geometry, now, we can explore the nature of the matter content of the star. In figure 5, pressure is plotted as a function of the energy density. This indicates a nearly linear relationship between pressure and energy density. In figure 6, the red (solid) line indicates the pressure-energy density curve which best fits with the broken black straight line given as $p_r = 0.4621\rho - 211$.

8. Mass-radius curve is also important for inferring the nature of the matter content of the star. Figure 7 shows the plot of the mass of the star in units of solar mass against the radius. The nature of the plot is consistent with the plots reported by previous studies.

9. Expression for the moment of inertia of compact astrophysical objects taking into consideration the effect of General Relativity is remarkably different from the expression for solid sphere given in mechanics. Using the slow rotation approximation proposed by Hartle [41], a number of attempts have been made for deriving an approximate expression for the moment of inertia of a compact star [42–44]. We use the approximate expression for the moment of inertia of the strange star provided in [45].

$$\mathcal{I} = 0.4(1 + \xi)MR^2 \tag{40}$$

Here, $\xi = \frac{M}{R}\frac{km}{M_\odot}$ is the dimensionless compactness parameter [46]. This value of the moment of inertia is valid up to the maximum mass of the star. In the next section, we plot $\mathcal{I}$ against the mass of the star (see figure 8). The plot clearly shows a maximum value for the moment of inertia with the increasing mass of the star.

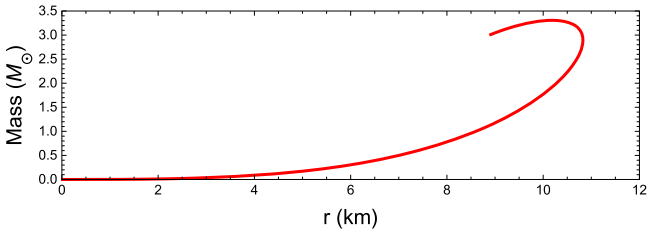

Figure 7. Mass-radius curve.

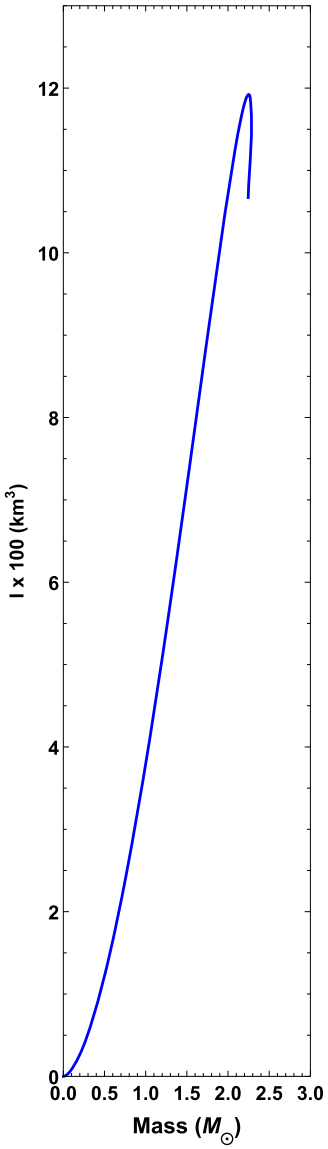

Figure 8. Variation of the moment of inertia of the star with mass.

8. Observational compatibility

The predicted values of mass and radius of the well-known pulsar 4U1820 − 30 are $M = 1.58\,M_\odot$ and $R = 9.1$ km, respectively [47]. Using these predicted values, one can immediately find out unknown constants α, β, F from equations (32)–(34) as follows: $\alpha = 1478.49$, $\beta = -1.11081$ and F=161.67 . Here, we assume $R = 30$. With the input of the calculated values of constants, we study the nature of

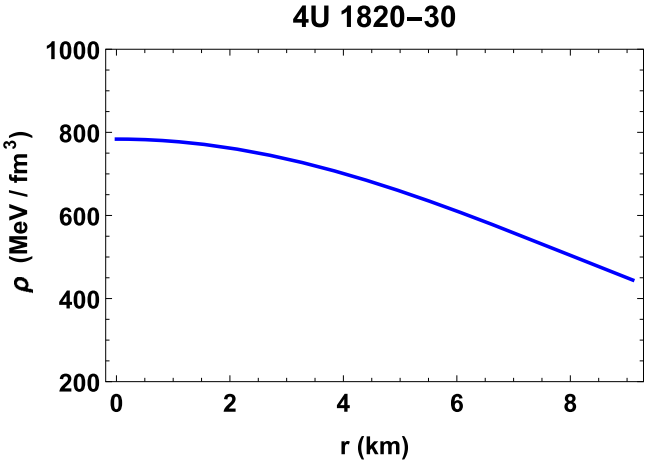

Figure 9. Fall-off behavior of energy density.

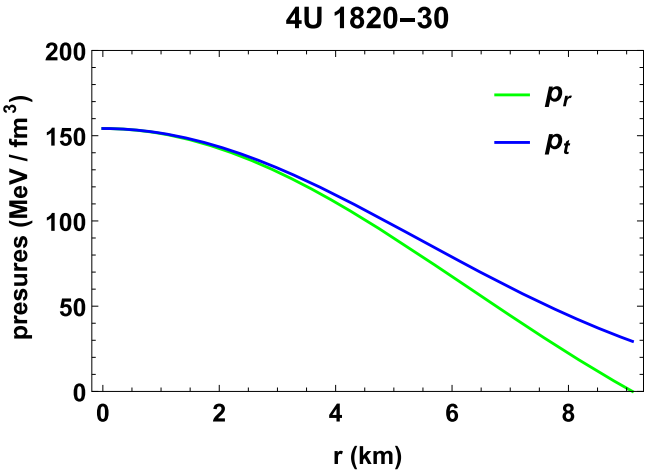

Figure 10. Fall-off behavior of radial and transverse pressure.

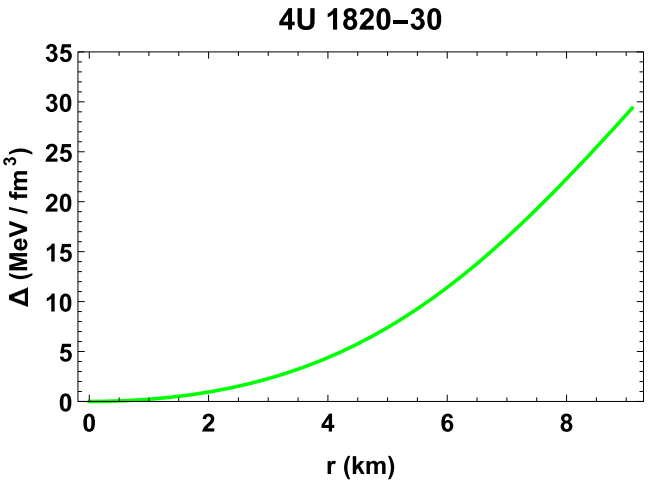

Figure 11. Radial variation of anisotropy.

different physical quantities in figures 9–12. In these plots, all physical quantities are expressed in usual C.G.S. units, substituting the values of G and c in proper places. The plots speak volumes about the physical viability of the model. Figure 9 shows that the density of the matter inside the star is

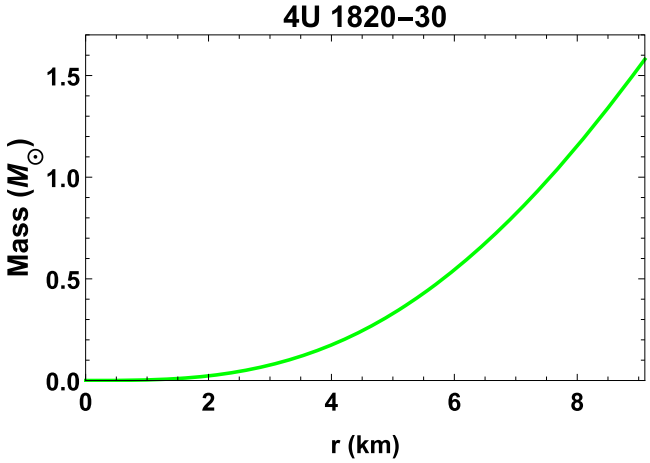

Figure 12. Verification of mass.

maximum at the center and it gradually decreases towards the boundary. Radial and tangential pressures are also maximum at the center and the plots gradually decline toward the boundary of the star (see figure 10). Though the tangential pressure doesn't vanish at the boundary, the radial pressure becomes zero at the boundary of the star. The anisotropy is zero at $r = 0$ and maximum at the surface of the star.

The mass function is increasing throughout the star and vanishes at $r = 0$ (see figure 12). Pressure expressed as a thermodynamic function of the energy density represents the equation of state (EOS) of the constituent matter inside the star. Figure 5 studies the nature of the EOS. The plot represents an almost linear EOS.

The model developed in the present paper can be useful in describing pulsars of varied masses. In table 1, we use the estimated values of masses and radii of RX J $1856-37$ [48], EXO $1785-248$ [49], Her X-1 [50], PSR J $1614-2230$, Cen X-3 and 4U $1608-52$ to study the values of important model parameters.

The values of the physical quantities at physically significant points of the tar are given in table 2. These values are sufficient to justify the applicability of the model. Here, the notations $()|_0$ and $()|_b$ are used to represent the calculated values of the physical parameters at the center and surface of the star, respectively.

9. Equilibrium under three different forces

The static equilibrium of an anisotropic star under the gravitational, hydro-static, and anisotropic forces may be described by the following equation:

$$-\frac{M_G(r)(\rho + p_r)}{r}e^{\frac{\nu-\lambda}{2}} - \frac{dp_r}{dr} + \frac{2}{r}(p_t - p_r) = 0, \qquad (41)$$

where $M_G(r)$ is the gravitational mass of the star within the radius r. Its value can be computed using the Tolman-Whittaker formula and the Einsteins field equations as follows:

$$M_G(r) = \frac{1}{2}re^{\frac{\lambda-\nu}{2}\nu'}. \qquad (42)$$

Table 1. Values of model parameters.

Pulsar	Mass ($M_\odot$)	Radius (km)	R	α	β	F
RX J 1856 − 37	0.9 ± 0.2	≈6	20	545.29	−0.7514	81.36
EXO 1785 − 248	1.3 ± 0.2	8.849 ± 0.4	34	2134.86	−1.2282	180.68
Her X-1	0.85 ± 0.15	8.1 ± 0.41	34	1687.83	−0.7169	211.94
PSR J 1614 − 2230	1.97 ± 0.04	9.69 ± 0.2	28	1202.03	−1.1091	156.56
Cen X-3	1.49 ± 0.08	9.178 ± 0.13	30	1310.32	−0.88439	175.88
4U1608 − 52	1.74 ± 0.14	9.52 ± 0.15	28	1053.33	−0.8403	168.08

Substituting the value of $M_G(r)$ in equation (41) we find

$$-\frac{\nu'}{2}(\rho + p_r) - \frac{\mathrm{d}p_r}{\mathrm{d}r} + \frac{2}{r}(p_t - p_r) = 0. \tag{43}$$

The above equation is equivalent to

$$F_g + F_h + F_a = 0, \tag{44}$$

where

$$F_g = -\frac{\nu'}{2}(\rho + p_r), \tag{45}$$

$$F_h = -\frac{\mathrm{d}p_r}{\mathrm{d}r}, \tag{46}$$

$$F_a = \frac{2}{r}(p_t - p_r). \tag{47}$$

Using the equations (23)–(25), the expression for F_g, F_h and F_a can be written in terms of model parameters as,

$$F_g = -\frac{1}{(r^8 - 4r^6R^2 + 6r^4R^4 + R^8 - 4r^2(R^6 - 4F\alpha^2))^2(\alpha + (-r^2 + R^2)\beta)^2} \times [8r(r^2 - R^2)^2\alpha^2(r^8 - 4r^6R^2 + R^8 + 8FR^2\alpha^2 + 8FR^4\alpha\beta + 6r^4(R^4 - 4F\alpha\beta) - 4r^2(R^6 - 10F\alpha^2 - 4FR^2\alpha\beta))], \tag{48}$$

$$F_h = \frac{-8\alpha r}{(16\alpha^2Fr^2 + (r^2 - R^2)^4)^2(\alpha + \beta(R^2 - r^2))^2} \times [((r^2 - R^2)^4 + 16Fr^2\alpha^2)(-\alpha + (r^2 - R^2)\beta) \times (3(r^2 - R^2)^2 - 4F\alpha\beta) - ((r^2 - R^2)^4 + 16Fr^2\alpha^2)\beta((r^2 - R^2)^3 + 4F\alpha^2 - 4F(r^2 - R^2)\alpha\beta) - 4((r^2 - R^2)^3 + 4F\alpha^2)(-\alpha + (r^2 - R^2)\beta)((r^2 - R^2)^3 + 4F\alpha^2 - 4F(r^2 - R^2)\alpha\beta)], \tag{49}$$

$$F_a = -\frac{2}{r(r^8 - 4r^6R^2 + 6r^4R^4 + R^8 - 4r^2(R^6 - 4F\alpha^2))^2(-\alpha + (r^2 - R^2)\beta)} \times (8r^2\alpha(r^6 - 3r^4R^2 + 3r^2R^4 - R^6 + 4F\alpha^2)(r^6 - 3r^4R^2 - R^6 + 8F\alpha^2 + 8FR^2\alpha\beta + r^2(3R^4 - 8F\alpha\beta)), \tag{50}$$

which represent the gravitational, hydrostatics and anisotropic forces, respectively.

The plot of the aforementioned forces is given in figure 13. The figure shows that the negativity of gravitational force is balanced by positive forces, like, hydro-static and anisotropic force and thereby maintaining the static equilibrium of the system.

10. Stability analysis of the model

10.1. Adiabatic index

The adiabatic index for the anisotropic star is given by the following equation:

$$\Gamma = \frac{\rho + p_r}{p_r}\frac{\mathrm{d}p_r}{\mathrm{d}\rho}, \tag{51}$$

This quantity is closely connected to an anisotropic star's stability. Researchers [51] have reported the value of the adiabatic index to remain in the range $\Gamma > \frac{4}{3}$ for the stable equilibrium of an isotropic sphere. Figure 14 shows the plot of Γ_r. It can be noted that Γ_r satisfies the requirement for stability everywhere inside the star.

10.2. Causality condition

In a realistic model of an anisotropic star, the sound speeds inside the star must be subluminal, i.e., $0 \leqslant \frac{\mathrm{d}p_r}{\mathrm{d}\rho} \leqslant 1$, $0 \leqslant \frac{\mathrm{d}p_t}{\mathrm{d}\rho} \leqslant 1$. This is termed the causality condition. Utilizing the 'cracking' concept proposed by Herrera [52], Abreau et. al [53] showed that the probable condition for a model of a compact star to be stable is $-1 \leqslant v_{st}^2 - v_{sr}^2 \leqslant 0$. Andréasson [54] modified this range as $0 < |v_{st}^2 - v_{sr}^2| < 1$. Figure 15 shows that the sound speeds are less than one inside the star.

Table 2. Values of physical quantities.

Pulsar	$\rho\|_0$	$\rho\|_b$	$\frac{dp_r}{d\rho}\|_0$	$\frac{dp_r}{d\rho}\|_b$	$\frac{dp_t}{d\rho}\|_0$	$\frac{dp_t}{d\rho}\|_b$	$(\rho+p_r+2p_t)\|_0$	$(\rho+p_r+2p_t)\|_b$
RX J 1856 − 37	1390	950	0.70	0.38	0.65	0.25	2012	1023
EXO 1785 − 248	674	411	0.38	0.29	0.32	0.18	931	462
Her X-1	496	382	0.48	0.33	0.41	0.21	614	416
PSR J 1614 − 2230	872	432	0.79	0.42	0.78	0.28	1670	508
Cen X-3	660	425	0.64	0.36	0.58	0.23	1035	469
4U 1608 − 52	716	425	0.87	0.41	0.84	0.27	1248	482

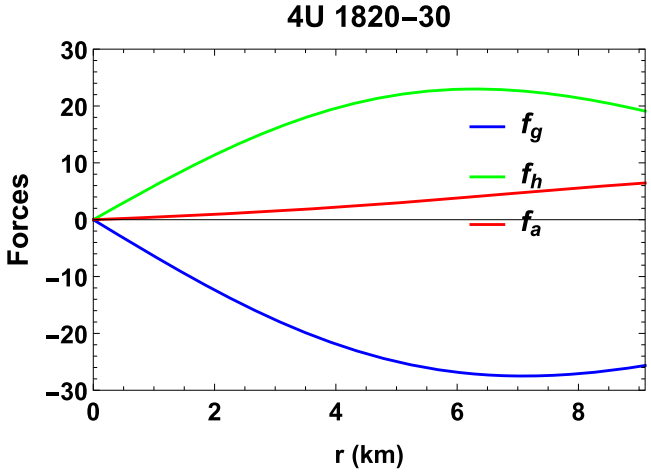

Figure 13. The variation of three different forces acting on the system is plotted against r.

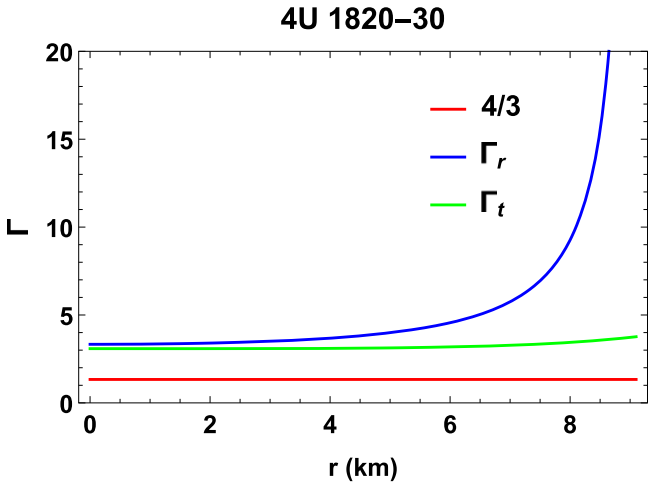

Figure 14. The relativistic adiabatic index plotted against r.

Therefore, the causality condition is satisfied throughout the star.

11. Discussions

In this paper, we have obtained an embedding class -I type interior solution to the Einstein field equations for an anisotropic matter distribution. This has been achieved by employing the Karmakar condition. The solutions we obtained are regular and well-behaved and could be used to describe a relativistic compact anisotropic star. All the physically relevant parameters e.g., metric potentials, density, pressures, mass, and anisotropy are positive and singularity free in every part of the star. The gradients of the matter variables are negative throughout the structure indicating that they pick a maximum value at the centre and gradually decrease towards the boundary of the star. One interesting feature of our approach is that we have not assumed any equation of state relating to the pressure and density of the matter composition of the star. Our approach enables us to find a relationship between these thermodynamical parameters. The relationship between the energy density and radial pressure which reflects the nature of the equation of state (EoS) of the matter distribution shows an almost linear relationship. The Karmakar condition allowed us to determine both the metric potentials and the nature of the EoS that can be predicted from the plot.

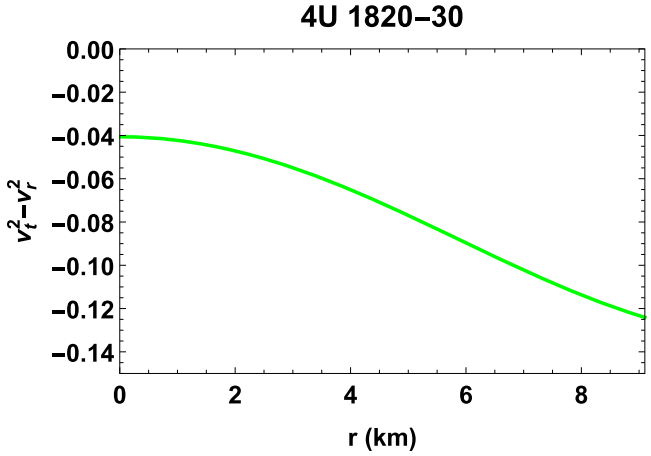

Figure 15. $v_t^2 - v_r^2$ is plotted against r.

The nature of the mass-radius curve obtained in the present study agrees very well with the plots reported in the literature. The plot of the moment of inertia against the mass of the star shows a maximum value for the moment of inertia with the increasing mass of the star.

A stable configuration demands that it should satisfy the TolmanOppenheimerVolkoff equilibrium condition. The stability of the model has been demonstrated graphically where the gravitational force is counterbalanced by the combined effect of the anisotropic and hydro-static force. A few other parameters that should be verified for stable conditions are

also checked here. We verify the sound speeds in both radial and transverse directions obey the corresponding limit. Further, Herrera's cracking condition has been verified in our proposed model.

It was first described by Chandrasekhar [55] that any stellar configuration will maintain its stability if the adiabatic index $\Gamma > 4/3$. This has been clearly shown graphically.

One interesting feature of the assumed metric of our model is that under a particular approximation, it is reduced to the well-known Tolman metric.

Acknowledgments

FR and SD would like to thank the authorities of the Inter-University Centre for Astronomy and Astrophysics, Pune, India for providing research facilities.

References

[1] Schwarzschild K 1916 On the gravitational field of a mass point according to einsteins theory *Sitzer. Preuss. Akad. Wiss, Berlin* 189
[2] Bowers R L and Liang E P T 1974 Spherical Gravitational collapse of anisotropic radiating fluid sphere *Astrophys. J.* **188** 657
[3] Ruderman R 1972 Pulsar: Structure and dynamics *Ann. Rev. Astron. Astrophys.* **10** 427
[4] Kippenhahn R and Weigert A 1990 *Stellar Structure and Evolution* (Berlin: Springer)
[5] Sokolov A I 1980 Phase Transitions in a superfluid neutron liquid *JETP* **79** 1137
[6] Sawyer R F 1972 Condensed PI- phase in neutron-star Matter *Phys. Rev. Lett.* **29** 382
[7] Herrera L and Santos N O 1995 Jeans mass for anisotropic matter *Astrophys. J.* **438** 308
[8] Letelier P 1980 Anisotropic fluids with two perfect fluid components *Phys. Rev.* D **22** 807
[9] Weber F 1999 *Pulsars as Astrophysical Observatories for Nuclear and Particle Physics Bristol* (Bristol: IOP Publishing)
[10] Thirukkanesh S and Ragel F C 2012 Exact anisotropic sphere with polytropic equation of state *Pramana J. Phys.* **78** 687
[11] Nilsson U S and Uggla C 2001 General Relativistic Stars: Polytropic equations of state *Ann. Phys.* **286** 292
[12] Heinzle J M, Röhr N and Uggla C 2003 *Class. Quantum Gravit.* **20** 4567
[13] Kinasiewicz B and Mach P 2007 From polytropic to barotropic perfect fluids in general relativistic hydrodynamics *Acta Phys. Pol.* B **38** 39–60
[14] Thirukkanesh S and Ragel F S 2014 Anisotropic spheres with Van der-Waals type equation of state *Pramana J. Phys.* **83** 83
[15] Morris M S and Thorne K S 1988 Wormholes in spacetime and their use for intersteller travel: A tool for teaching general relativity *Am. J. Phys.* **56** 395
[16] Cattoen C, Faber T and Visser M 2005 Visser, Gravastars must have anisotropic pressures *Class. Quantum Gravity* **22** 4189
[17] DeBenedictis A, Horvat D, Ilijic S, Kloster S and Viswanathan K 2006 Gravastar solutions with continuous presures and equation of state *Class. Quantum Gravity* **23** 2303
[18] Das S, Parida B K and Sharma R 2022 Estimating tidal Love number of a class of compact star *Eur. Phys. J.* C **82** 136
[19] Das S, Ray S, Khlopov M, Nandi K K and Parida B K 2021 Anisotropic Compact Stars: Constraining model parameter to account for physical features of tidal love numbers *Anns. of Phys.* **433** 168597
[20] Bhar P, Das S and Parida B K 2022 Compact stellar model in tolman space-time in presence of pressure anisotropy *Int. J. Geom. Methods Mod. Phys.* **19** 2250095
[21] Gedela S, Pant N, Upreti J and Pant R P 2019 Relativistic core-envelope anisotropic fluid model of super dense star *Eur. Phys. J.* C **79** 566
[22] Pant N, Gedela S, Pant R P, Upreti J and Bisht R K 2020 *Eur. Phys. J. Plus* **135** 180
[23] Karmarkar K R 1948 Gravitational metrices of spherical symmetry and class one *Proc. Ind. Acad. Sci.* A **27** 56
[24] Prasad A K, Kumar J, Maurya S K and Dayanandan B 2019 Relativistic model for anisotropic compact stars using karmakar condition Astrophys *Space Sc.* **364** 66
[25] Maurya S K, Deb D, Ray S and Kuhfittig P K F 2019 A study of anisotropic compact star based on embedding class 1 condition *Int. J. Mod. Phys.* D **28** 1950116
[26] Pant N, gedela S and Bisht R K 2021 Stellar modeling with the Einstein-Maxwell field equations via gravitational decoupling *Chinese J. Phys.* **72** 530
[27] Gedela S, Bisht R K and Pant N 2020 Relativistic modeling of stellar object using embedded class one spacetime continuum *Mod. Phys. Lett.* A **35** 2050097
[28] Sagar K G, Pandey B and Pant N 2022 *Astrphys. Space Sc.* **367** 72
[29] Bhar P, Maurya S K, Gupta Y K and Manna T 2016 Modelling of anisotropic compact stars of embedding class one *Eur. Phys. J.* A **52** 312
[30] Maurya S K, Gupta Y K, Smitha T T and Rahaman F 2016 A new exact solution for anisotropic compact stars of embedding class one arXiv:1512.01667*Eur. Phys. J. A* **7** 191
[31] Maurya S K, Ratanpal B S and Govender M 2017 Anisotropic stars for spherically symmetric spacetimes satisfying the Karmakar condition *Ann. of Phys.* **382** 36
[32] Maurya S K and Maharaj S D 2017 Anisotropic fluid spheres of embedding class one using Karmakar condition *Eur. Phys. J.* C **77** 328
[33] Maurya S K, Gupta Y K, Ray S and Roychoudhury S Spherically symmetric electromagnetic mass models of embedding class one arXiv:1506.02498
[34] Maurya S K, Gupta Y K, Ray S and Deb D 2017 A new model for spherically symmetric charged compact stars of embedding class 1 *Eur. Phys. J.* C **77** 45
[35] Maurya S K and Govender M 2018 *Eur. Phys. J.* A **54** 68
[36] Deb D, Ghosh S, Maurya S K, Khlopov M and Ray S Anisotropic compact stars in f(T) gravity under Karmakar condition arXiv:1811.11797
[37] Pant N, Gedela S, Ray S and Sagar K G 2022 Relativistic charged stellar model of the Pant interior solution via gravitational decoupling and Karmakar conditions *Mod. Phys. Lett.* A **37** 2250072
[38] Das S, Rahaman F and Baskey L 2019 A new class of compact stellar model compatible with observational data *Eur. Phys. J.* C **79** 853
[39] Pandey S N and Sharma S P 1981 Insufficiency of Karmakar's condition *Gen. Relativ. Gravit.* **14** 113
[40] Tolman R C 1939 Static solution of einstein's field equation for spheres of fluid *Phys. Rev.* **55** 364
[41] Hartle J B 1967 Slowly rotating relativistic stars I. equations of structure *Astrophys. J.* **150** 1005
[42] Lattimer J M and Schutz B F 2005 Constraining the equation of state with moment of inertia measurements *Astrophys. J.* **629** 979

[43] Lattimer J M and Prakash M 2007 Neutron star observations: Prognosis for equation of state constraints *Phys. Rep.* **442** 109
[44] Raithel C A, Özel F and Psaltis D 2016 Model-independent inference of neutron star radii from moment of inertia measurement *Phys. Rev.* C **93** 032801
[45] Bejger M and Hansel P 2002 Moment of inertia for neutron and strange stars: Limit derived for the crab pulsar *Astron. Astrophys.* **396** 917
[46] Ravenhall D G and Pethick C J 1994 Neutron star moments of inertia *Astrophys. J.* **424** 846
[47] Gangopadhyay T, Ray S, Li X-D, Dey J and Dey M 2013 Strange star equation of state fits the refined mass measurement of 12 pulsars and predicts their radii *Mon. Not. R. Astron. Soc.* **431** 3216
[48] Pons J A, Walter F M, Lattimer J M, Prakash M, Neuhauser R and An P 2002 Towards a mass and radius determination of the nearby isolated neutron star RX J185635-3754 *Astrophys. J.* **564** 981
[49] Özel F, Güver T and Pslatis D 2009 The mass and radius of the neutron star in EXO 1745-248 *Astrophys. J.* **693** 1775
[50] Abubekerov M K, Antokhina E A, Cherepashchuk A M and Shimanskii V V 2008 About the mass of the compact object in the X-ray binary Her X-1/HZ her *Astron. Rep.* **52** 379
[51] Heintzmann H and Hillebrandt W 1975 Neutron stars with an anisotropic equation of state: mass, redshift and stability *Astron. Astrophys.* **38** 51
[52] Herrera L 1992 Cracking of self-gravitating compact objects *Phys. Lett.* A **165** 206
[53] Abreu H, Hernández H and Núñez L A 2007 Sound speeds, cracking and stability of self-gravitating anisotropic compact object *Class. Quantum Gravity* **24** 4631
[54] Andréasson H 2009 Sharp bounds on the critical stability radius for relativistic charged spheres *Commun. Math. Phys.* **288** 715
[55] Chandrasekhar S 1964 The dynamical instability of gaseous masses approaching the schwarzschild limit in general relativity *Astrophys. J.* **140** 417